Synthesis and Properties of Octaethylporphinato(arenethiolato)iron(III) Complexes with Intramolecular NH···S Hydrogen Bond: Chemical Function of the Hydrogen Bond

Norikazu Ueyama,*,† Nami Nishikawa,† Yusuke Yamada,† Taka-aki Okamura,† Shigenori Oka,‡ Hiromu Sakurai,‡ and Akira Nakamura*,†

Department of Macromolecular Science, Graduate School of Science, Osaka University, Toyonaka, Osaka 560, Japan, and Department of Analytical and Bioinorganic Chemistry, Kyoto Pharmaceutical University, Yamashina, Kyoto 607, Japan

Received September 5, 1997

Iron(III) porphinate complexes of arenethiolate having single or double NH···S hydrogen bonds at the axial position, [Fe^{III}(OEP){S-2,6-$(RCONH)_2C_6H_3$}] (R = CF_3 (**1**), CH_3 (**2**)) or [Fe^{III}(OEP)(S-2-$RCONHC_6H_4$)] (R = CF_3 (**3**), CH_3 (**4**), *t*-Bu (**5**)), were synthesized as models of P-450 and chloroperoxidase. The presence of an NH···S hydrogen bond in these complexes is confirmed by their crystal structures in the solid state, the IR shift of the amide NH band and the direct through-bond contact-shift of the amide ^2H NMR signal in benzene. The NH···S hydrogen bond elongates the Fe−S bond distance, stabilizes the Fe(III) state, protects the complexes from decomposition by air and moisture, and shifts the redox to more positive potentials. These functions by the hydrogen bond are more significant than the effect of steric hindrance.

Introduction

The crystallographical structures of four different monooxidase cytochrome P-450s have been reported, for example, P-450cam,[1,2] P-450 BM-3,[3] P-450terp,[4] and P-450 eryF.[5] The analysis of coordination environments around the active site of P-450s obtained from the Protein Data Bank taught us that an invariant amino acid fragment, Cys-X-Gly-Y (X and Y are amino acid residues), exists at the axial position of the porphinato ligand. The Cys sulfur is surrounded by the amide NHs of the X-Gly-Y. Recently, the presence of NH···S hydrogen bond has been discussed in the active site of P-450cam[6,7] although the amide NHs of Leu-Gly-Gln are not directed toward the sulfur atom as shown in Figure 1a. There is a probability that the active site of P-450 has an NH···S hydrogen bond in solution.

On the other hand, the analysis of the crystal structure of chloroperoxidase (CPO) has demonstrated that a Cys-Pro-Ala-Leu at the axial position has two clear NH···S hydrogen bonds between Cys S and Ala NH and between Cys S and Leu NH (Figure 1b).[6] The presence of Pro residue probably promotes the formation of the NH···S hydrogen bond. However, no report has been published on the chemical function of the NH···S hydrogen bond.

Various thiolate Fe(III) complexes have been synthesized as models of P-450, mainly arenethiolate complexes.[8−15] Alkanethiolate model complexes are unstable because the dissociating thiolate ligand reduces the Fe(III) complex as a strong reductant to give an Fe(II) species. These Fe(III) model complexes are unstable against air or moisture. One exception has been reported for an Fe(III) complex having alkanethiolate tethered to the porphinate ring as reported by Higuchi et al.[16,17] The stability for the active center of P-450s and for the model complex has been hitherto considered to come from the steric hindrance around the thiolate.

The regulation of redox potential is crucial for the catalytic oxidation cycle in P450s. When a substrate binds the active site in P-450 cam, the redox potential shifts to the positive side to be readily reduced by a physiological reductant, for example, reduced putidaredoxin. The origin of the shift has been proposed to be the change of the spin state of the iron center.[18]

† Osaka University.
‡ Kyoto Pharmaceutical University.

(1) Poulos, T. L.; Finzel, B. C.; Howard, A. J. *Biochemistry* **1986**, *25*, 5314−5322.
(2) Poulos, T. L.; Finzel, B. C.; Howard, A. J. *J. Mol. Biol.* **1987**, *195*, 687−700.
(3) Li, H.; Poulos, T. L. *Acta Crystallogr.* **1995**, *D51*, 21−32.
(4) Hasemann, C. A.; Ravichandran, K. G.; Peterson, J. A.; Deisenhofer, J. *J. Mol. Biol.* **1994**, *236*, 1169−1185.
(5) Cupp-Vickery, J. R.; Poulos, T. L. *Nat. Struct. Biol.* **1995**, *2*, 144−153.
(6) Sundaramoorthy, M.; Terner, J.; Poulos, T. L. *Structure* **1995**, *3*, 1367−1377.
(7) Poulos, T. L. *J. Biol. Inorg. Chem.* **1996**, *1*, 356−359.
(8) Collman, J. P.; Sorrell, T. N.; Hoffman, B. M. *J. Am. Chem. Soc.* **1975**, *97*, 913−914.
(9) Dawson, J. H.; Holm, R. H.; Trudell, J. R.; Barth, G.; Linder, R. E.; Bunnenberg, E.; Djerassi, C.; Tang, S. C. *J. Am. Chem. Soc.* **1976**, *98*, 3707−3709.
(10) Koch, S.; Tang, S. C.; Holm, R. H. *J. Am. Chem. Soc.* **1975**, *97*, 916−917.
(11) Koch, S.; Tang, S. C.; Holm, R. H. *J. Am. Chem. Soc.* **1975**, *97*, 914−916.
(12) Miller, K. M.; Strouse, C. E. *Acta Crystallogr.* **1984**, *C40*, 1324−1327.
(13) Oshio, H.; Ama, T.; Watanabe, T.; Nakamoto, K. *Inorg. Chim. Acta* **1985**, *96*, 61−66.
(14) Miller, K. M.; Strouse, C. E. *Inorg. Chem.* **1984**, *23*, 2395−2400.
(15) Tang, S. C.; Koch, S.; Papaefthymiou, G. C.; Foner, S.; Frankel, R. B.; Ibers, J. A.; Holm, R. H. *J. Am. Chem. Soc.* **1976**, *98*, 2414−2434.
(16) Higuchi, T.; Uzu, S.; Hirobe, M. *J. Am. Chem. Soc.* **1990**, *112*, 7051−7053.
(17) Higuchi, T.; Shimada, K.; Maruyama, N.; Hirobe, M. *J. Am. Chem. Soc.* **1993**, *115*, 7551−7552.
(18) Fisher, M. T.; Sligar, S. G. *J. Am. Chem. Soc.* **1985**, *107*, 5018−5019.

S0020-1669(97)01140-3 CCC: $15.00 © 1998 American Chemical Society
Published on Web 04/21/1998

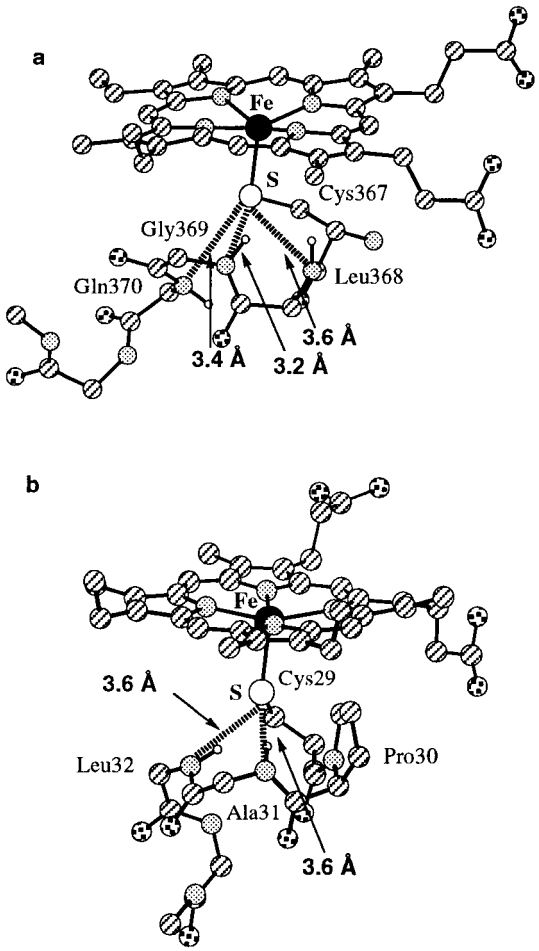

Figure 1. Crystal structures of (a) the active site of P-450cam[1] and (b) the active site of chloroperoxidase (CPO).[6]

Recently, amino acid substitution at the position of Arg^{112} has been reported to affect the redox potential due to electrostatic effects.[19,20]

We have been investigating the remarkable influence of NH···S hydrogen bonds at the active site of ferredoxins and in the related model complexes.[21] To investigate the chemical function of the NH···S hydrogen bond, novel arenethiolate ligands having intramolecular NH···S hydrogen bonds were designed. Thus, octaethylporphinato Fe(III) complexes of these ligands, $[Fe^{III}(OEP)\{S\text{-}2,6\text{-}(RCONH)_2C_6H_3\}]$ (R = CF_3 (**1**), CH_3 (**2**)) and $[Fe^{III}(OEP)(S\text{-}2\text{-}RCONHC_6H_4)]$ (R = CF_3 (**3**), CH_3 (**4**), *t*-Bu (**5**)), were synthesized and compared with simple thiolate complexes, for example, $[Fe^{III}(OEP)(SPh)]$ (**6**), $[Fe^{III}(OEP)(S\text{-}2\text{-}CH_3C_6H_4)]$ (**7**), $[Fe^{III}(OEP)(S\text{-}2,4,6\text{-}Me_3C_6H_2)]$ (**8**), and $[Fe^{III}(OEP)(S\text{-}4\text{-}CF_3CONHC_6H_4)]$ (**9**). The difference in the crystal structures between these complexes has been communicated.[22] A detailed description of the properties of these complexes is presented in this paper.

Experimental Section

Materials. All procedures were performed under an argon atmosphere by the Schlenk technique, except for ligand syntheses. All solvents were dried and distilled under an argon atmosphere before use. $[Fe^{III}(OEP)Cl]$ was obtained from Aldrich Chemical Co., Inc. $[Fe^{III}(OEP)]_2O$ was synthesized by the same method as $[Fe^{III}(TPP)]_2O$.[23] $[Fe^{III}(OEP)(SPh)]$ was synthesized by the reported methods.[15] Bis-[2,6-bis(trifluoroacetylamino)phenyl] disulfide, bis[2,6-di(acetylamino)-phenyl] disulfide, bis(2-trifluoroacetylaminophenyl) disulfide, bis(2-acetylaminophenyl) disulfide, and bis(2-pivaloylaminophenyl) disulfide were synthesized by literature methods.[24,25]

$[Fe^{III}(OEP)\{S\text{-}2,6\text{-}(CF_3CONH)_2C_6H_3\}]$ (1). $[Fe^{III}(OEP)(SPh)]$ (OEP = octaethylporphinato) (27 mg, 3.9×10^{-2} mmol) and $\{S\text{-}2,6\text{-}(CF_3CONH)_2C_6H_3\}_2$ (16 mg, 2.4×10^{-2} mmol) were suspended in 2 mL of toluene. The reaction mixture was stirred for 1 h at 60 °C, and then all reactants dissolved. The product was collected by filtration from the cooled reaction mixture, washed with *n*-hexane, and dried in vacuo, affording black microcrystals. The crystals used in X-ray study were collected from the concentrated mother liquor. Yield: 16 mg (44%). Anal. Calcd for $C_{46}H_{49}N_6O_2F_6FeS\cdot(C_7H_8)_{0.5}$: C, 61.55; H, 5.53; N, 8.70. Found: C, 61.08; H, 5.78; N, 8.54.

$[Fe^{III}(OEP)\{S\text{-}2,6\text{-}(CH_3CONH)_2C_6H_3\}]$ (2). $[Fe^{III}(OEP)(SPh)]$ (38 mg, 5.4×10^{-2} mmol) and $\{S\text{-}2,6\text{-}(CH_3CONH)_2C_6H_3\}_2$ (13 mg, 3.0×10^{-2} mmol) were suspended in 2 mL of toluene. The reaction mixture was stirred for 1 h at 70 °C. After the reaction mixture had cooled, the product was collected by filtration, washed with *n*-hexane, and dried in vacuo, affording black microcrystals. Yield: 15 mg (34%). Anal. Calcd for $C_{46}H_{55}N_6O_2FeS\cdot(C_7H_8)_{0.5}$: C, 69.30; H, 6.93; N, 9.80. Found: C, 69.44; H, 6.84; N, 9.60.

$[Fe^{III}(OEP)(S\text{-}2\text{-}CF_3CONHC_6H_4)]$ (3). $[Fe^{III}(OEP)]_2O$ (31 mg, 2.6×10^{-2} mmol) and $2\text{-}CF_3CONHC_6H_4SH$ (52 mg, 2.4×10^{-1} mmol) were suspended in 5 mL of toluene. The reaction mixture was stirred for 1 h at 60 °C and allowed to cool slowly. Black microcrystals were collected. The crystals used in the X-ray study were obtained from the concentrated mother liquor. Yield: 22 mg (53%). Anal. Calcd for $C_{44}H_{49}N_5OF_3FeS\cdot(C_7H_8)_{0.5}$: C, 66.74; H, 6.25; N, 8.19. Found: C, 66.32; H, 6.19; N, 9.19.

$[Fe^{III}(OEP)(S\text{-}2\text{-}CH_3CONHC_6H_4)]$ (4). $[Fe^{III}(OEP)]_2O$ (32 mg, 2.7×10^{-2} mmol) and $2\text{-}CH_3CONHC_6H_4SH$ (33 mg, 2.0×10^{-1} mmol) were suspended in 2 mL of toluene. The reaction mixture was heated to 70 °C for a short period and then allowed to cool slowly. The product was collected to afford dark brown microcrystals which were washed with *n*-hexane and dried in vacuo. Yield: 20 mg (54%). Anal. Calcd for $C_{36}H_{44}N_4OFeS$: C, 70.01; H, 6.94; N, 9.28. Found: C, 69.72; H, 6.93; N, 9.26.

$[Fe^{III}(OEP)(S\text{-}2\text{-}t\text{-}BuCONHC_6H_4)]$ (5). $[Fe^{III}(OEP)]_2O$ (30 mg, 2.5×10^{-2} mmol) and $2\text{-}t\text{-}BuCONHC_6H_4SH$ (27 mg, 1.3×10^{-1} mmol) were suspended in 2 mL of toluene. The reaction mixture was stirred for 30 min at 60 °C. The product was collected from the cooled reaction mixture, washed with *n*-hexane, and dried in vacuo, giving black microcrystals. Yield: 16 mg (40%). Anal. Calcd for $C_{36}H_{44}N_4OFeS$: C, 70.01; H, 6.94; N, 9.28. Found: C, 69.72; H, 6.93; N, 9.26.

$[Fe^{III}(OEP)(S\text{-}2\text{-}CH_3C_6H_4)]$ (7). $[Fe^{III}(OEP)]_2O$ (30 mg, 2.5×10^{-2} mmol) and *o*-toluenethiol (60 μL, 0.51 mmol) were dissolved and stirred in 5 mL of toluene at 70 °C for 1 h. After the solution was cooled to 3 °C, black microcrystals were obtained. Anal. Calcd for $C_{45}H_{55}N_4FeS$: C, 73.05; H, 7.49; N, 7.57. Found: C, 73.06; H, 7.47; N, 7.53.

$[Fe^{III}(OEP)(S\text{-}2,4,6\text{-}Me_3C_6H_2)]$ (8). $[Fe^{III}(OEP)]_2O$ (40 mg, 3.4×10^{-2} mmol), 2,4,6-trimethylbenzenethiol (99 mg, 0.65 mmol) and bis-(2,4,6-trimethylphenyl) disulfide (80 mg, 0.26 mmol) were dissolved, and the mixture was stirred in toluene at 60 °C for 15 min. After the solution was cooled to 3 °C, black needle crystals were obtained. Anal. Calcd for $C_{45}H_{55}N_4FeS$: C, 73.05; H, 7.49; N, 7.57. Found: C, 73.06; H, 7.47; N, 7.53.

(19) Koga, H.; Sagara, Y.; Yaoi, T.; Tsujimura, M.; Nakamura, K.; Sekimizu, K.; Makino, R.; Shimada, H.; Ishimura, Y.; Yura, K.; Go, M.; Ikeguchi, M.; Horiuchi, T. *FEBS Lett.* **1993**, *331*, 109−113.
(20) Unno, M.; Shimada, H.; Toba, Y.; Makino, R.; Ishimura, Y. *J. Biol. Chem.* **1996**, *271*, 17869−17874.
(21) Ueyama, N.; Yamada, Y.; Okamura, T.; Kimura, S.; Nakamura, A. *Inorg. Chem.* **1996**, *35*, 6473−6484.
(22) Ueyama, N.; Nishikawa, N.; Yamada, Y.; Okamura, T.; Nakamura, A. *J. Am. Chem. Soc.* **1996**, *118*, 12826−12827.
(23) Fleischer, E. B.; Srivastava, T. S. *J. Am. Chem. Soc.* **1969**, *91*, 2403−2404.
(24) Okamura, T.; Takamizawa, S.; Ueyama, N.; Nakamura, A. *Inorg. Chem.* **1998**, *37*, 18−28.
(25) Ueyama, N.; Okamura, T.; Yamada, Y.; Nakamura, A. *J. Org. Chem.* **1995**, *60*, 4893−4899.

Table 1. Crystallographic Data for $[Fe^{III}(OEP)\{S\text{-}2,6\text{-}(CF_3CONH)_2C_6H_3\}]\cdot{}^1/_2$toluene (**1**) and $[Fe^{III}(OEP)(S\text{-}2\text{-}CF_3CONHC_6H_4)]\cdot{}^1/_2$toluene (**3**)

parameter	**1**	**3**
empirical formula	$C_{49.50}H_{53}N_6O_2SF_6Fe$	$C_{47.50}H_{53}N_5OF_3SFe$
fw	965.90	854.88
crystal system	triclinic	triclinic
a, Å	13.304(4)	13.467(4)
b, Å	20.151(5)	14.797(6)
c, Å	9.201(2)	12.821(5)
α, deg	90.82(2)	103.88(3)
β, deg	101.77(2)	107.71(3)
γ, deg	100.65(2)	65.94(2)
V, Å^3	2369(1)	2202(1)
space group	$P\bar{1}$	$P\bar{1}$
Z	2	2
ρ_{calc}, g cm^{-1}	1.354	1.289
μ, cm^{-1}	4.31	4.43
$R(F_o)^a$	0.063	0.069
$R_w(F_o)^b$	0.069	0.068
no. of measd reflcns	8725	9625
no. of unique reflcns	8329	9193
no. of reflcns obsd ($I > 3\sigma(I)$)	2965	2329
goodness of fit^c	1.81	1.83

^{a} $R = \sum(|F_o| - |F_c|)/\sum|F_o|$. ^{b} $R_w = \{\sum w(|F_o| - |F_c|)^2/\sum w|F_o|^2\}^{1/2}$, $w = 1/\sigma^2(F_o)$. ^{c} GOF $= \{\sum(|F_o| - |F_c|)/\sigma\}/(n - m)$, where *n* is the number of reflections used in the refinement and *m* is the number of variables.

$[Fe^{III}(OEP)(S\text{-}4\text{-}CF_3CONHC_6H_4)]$ (9). $[Fe^{III}(OEP)]_2O$ (40 mg, 3.4 $\times$ 10^{-2} mmol) and 4-$CF_3CONHC_6H_4SH$ (37 mg, 0.17 mmol) were suspended in 2 mL of toluene. The reaction mixture was stirred for 2 h at 50 °C. The solution was concentrated and allowed to cool slowly. Black microcrystals were collected. Anal. Calcd for $C_{44}H_{49}N_5OF_3FeS$: C, 65.34; H, 6.11; N, 8.66. Found: C, 63.46; H, 5.79; N, 8.21.

Preparation of N^{2}H-Substituted Fe(III) Porphinate Complexes. The amide N^{2}H-substituted arenethiolate ligands were obtained by the amide NH exchange of the arenethiolate or diaryl disulfide with methanol-d_1. N^{2}H-substituted Fe(III) porphinate complexes were obtained by the reaction of $[Fe^{III}(OEP)(SPh)]$ with the corresponding amide N^{2}H-substituted arenethiol or by reaction of $[Fe^{III}(OEP)]_2O$ with the corresponding amide N^{2}H-substituted aryl disulfide by the same method as previously described for the syntheses of complexes **1** and **3**.

Preparation of an Aqueous Micellar Solution of $[Fe^{III}(OEP)\{S\text{-}2,6(CF_3CONH)_2C_6H_3\}]$. $[Fe^{III}(OEP)\{S\text{-}2,6\text{-}(CF_3CONH)_2C_6H_3\}]$ (1.73 mg, 1.79 $\times$ 10^{-3} mmol) was dissolved in 0.90 mL of toluene, and 0.90 mL of Triton X-100 was added to the solution. After the toluene was removed in vacuo, the solution was diluted with 8.1 mL of water to give a homogeneous 0.2 mM aqueous micellar solution.

Physical Measurements. Absorption spectra were recorded on a Shimadzu UV-3100PC spectrophotometer using a 1-mm cell. ^{1}H NMR spectra were measured on a JEOL EX270 spectrometer. The recycle delay used was 0.1 s. ^{2}H NMR spectra measurements were carried out in benzene on a JEOL JNM-LA 500 NMR spectrometer. IR spectra were obtained using KBr pellets on a Jasco FT/IR-8300 spectrometer. The cyclic voltammograms were recorded on a BAS 100B/W instrument with a three-electrode system consisting of a glassy carbon working electrode, a platinum-wire counter electrode, and a saturated calomel electrode (SCE). The scan rate was 100 mV/s. The sample concentration was 2.5 mM in CH_2Cl_2, containing 0.2 M of *n*-Bu_4NClO_4 as supporting electrolyte. Potentials were determined at room temperature vs SCE as a reference.

X-ray Structure Determination. Single crystals of $[Fe^{III}(OEP)\{S\text{-}2,6\text{-}(CF_3CONH)_2C_6H_3\}]$ (**1**) and $[Fe^{III}(OEP)(S\text{-}2\text{-}CF_3CONHC_6H_4)]$ (**3**) were sealed in a glass capillary. The X-ray data were collected at 23 °C on a Rigaku AFC7R (for **1**) and AFC5R (for **3**) diffractometer equipped with a rotating anode X-ray generator. The radiation used was Mo Kα monochromatized with graphite (0.710 69 Å). An empirical absorption correction was applied. The basic crystallographic parameters for **1** and **3** are listed in Table 1. Unit cell dimensions were refined by 25 reflections. These standard reflections were chosen and monitored with every 150 reflection and did not show any significant change. The structures were solved by a Patterson method and expanded using Fourier techniques. Some non-hydrogen atoms were refined anisotropically, while the rest were refined isotropically. Hydrogen atoms were included but not refined.

Results

Synthesis. The Fe(III) porphinate complexes of arenethiolate having two acylamino groups at the 2,6-positions of the arenethiolate, $[Fe^{III}(OEP)\{S\text{-}2,6\text{-}(RCONH)_2C_6H_3\}]$ (R = CF_3 (**1**), CH_3 (**2**)), were synthesized by a ligand exchange reaction between disulfide and $[Fe^{III}(OEP)(SPh)]$ (**6**). Other Fe(III) porphinate thiolate complexes with one acylamide group at the 2-position of the arenethiolate, $[Fe^{III}(OEP)(S\text{-}2\text{-}RCONHC_6H_4)]$ (R = CF_3 (**3**), CH_3 (**4**), *t*-Bu (**5**)), were synthesized by a similar ligand exchange reaction between $[Fe(OEP)]_2O$ and the corresponding thiol as reported in the literature.[15]

$$[Fe^{III}(OEP)(SPh)] + {}^1/_2ArSSAr \rightarrow [Fe^{III}(OEP)(SAr)] + {}^1/_2PhSSPh \quad (1)$$

$$[Fe(OEP)]_2O + 2ArSH \rightarrow 2[Fe^{III}(OEP)(SAr)] + H_2O \quad (2)$$

The reported method (eq 2) for the synthesis of arenethiolate model complexes is a ligand exchange reaction between the μ-oxo porphinate dimer and the thiol. In this case, a large excess of the thiol and the disulfide is required as a redox buffer to avoid the reduction of the thiolate Fe(III) complexes.[26] The introduction of a nitro group at the 4-position of arenethiolate promotes the formation of Fe(III) complexes only in the presence of an excess of the thiol even without the disulfide.[15] Our Fe(III) porphinato thiolate complexes were prepared by the reaction between the μ-oxo porphinate dimer and the equimolar thiol. Such a ligand exchange reaction was facilitated by the higher acidity of the thiols than the benzenethiol. Although the amide group at the 2-position of the arenethiolato ligand has only a weak electronic effect as indicated in its Hammett σ_p value = 0,[27] the adjacent amide group to SH increases the acidity of the thiol in the present case. For example, 2-$CH_3CONHC_6H_4SH$ shows lower pK_a value (5.7) compared with benzenethiol (8.0).[28] On the other hand, the complexes **1** and **2** were synthesized by the redox-driven ligand exchange reaction of $[Fe^{III}(OEP)(SPh)]$ with the corresponding disulfide. The reaction was controlled by the difference of the redox potentials between ArSSAr and PhSSPh.[24]

X-ray Analysis of 1 and 3. Table 2 lists the selected bond lengths and bond angles, and Figure 2 shows these structures. Each thiolate binds at the axial position of Fe(III) porphinate to give the 5-coordinated complexes. These crystals contain a half of the toluene molecule for each molecule, being coincident with the results of elemental analysis. Two NH protons turn to the direction of the neighboring sulfur atom with the distances (2.96 Å) between amide N and S in **1**. The NH proton in **3** also faces to the sulfur atom with a distance of 2.93 Å. **1** has

(26) Byrn, M. P.; Strouse, C. E. *J. Am. Chem. Soc.* **1991**, *113*, 2501−2508.
(27) Jaffe, H. H. *Chem. Rev.* **1953**, *53*, 191.
(28) Ueyama, N.; Moriyama, S.; Yamada, Y.; Inohara, M.; Ueno, T.; Okamura, T.; Nakamura, A., to be submitted.

Table 2. Selected Distances (Å) and Angles (deg) in [Fe^{III}(OEP){*S*-2,6-$(CF_3CONH)_2C_6H_3$}] (**1**), [Fe^{III}(OEP)(*S*-2-$CF_3CONHC_6H_4$)] (**3**), and [Fe^{III}(OEP)(SPh)] (**6**)

	1[a]	**3**[a]	**6**[b]
Fe−S (Å)	2.356(3)	2.327(4)	2.299(3)
Fe−N(mean) (Å)	2.048	2.04	2.057
Fe−N_4 (Å)	0.4142	0.3862	0.466(1)
Fe−S−C (deg)	104.5(3)	104.0(5)	102.5(3)
Fe−S−C−C (deg)	91.2(8)	104(1)	95.0
N- - -S (Å)	2.962(9)	2.93(1)	
	2.956(9)		
NH···S (Å)	2.419	2.390	
	2.434		

[a] This work. [b] Data from ref 12.

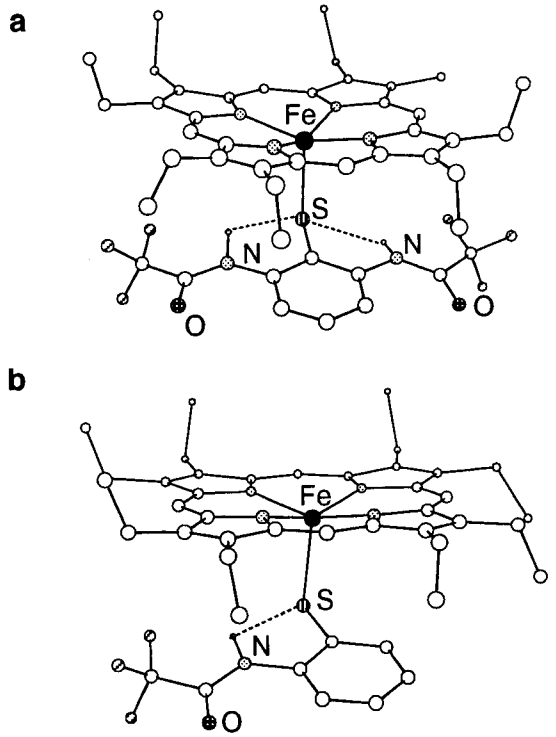

Figure 2. Crystal structures of (a) doubly NH···S hydrogen-bonded [Fe^{III}(OEP){S-2,6-$(CF_3CONH)_2C_6H_3$}] (**1**) and (b) singly NH···S hydrogen-bonded [Fe^{III}(OEP)(S-2−$CF_3CONHC_6H_4$)] (**3**).

an Fe−S bond distance of 2.356(3) Å, longer by 0.029 Å than that (2.327(4) Å) in **3** and longer by 0.057 Å than that (2.299 Å) in **6**.

Detection of Hydrogen Bond by IR Spectra. The formation of the NH···S hydrogen bond in the solid state was determined using IR spectroscopic measurements. Amide bands of corresponding diaryl disulfides were employed as standard values for ν(NH) and ν(C═O) stretchings in solution. Dichloromethane is used as a weakly polar solvent that does not strongly solvate intermolecularly with the amide group over a concentration range of 5−20 mM. Table 3 lists the IR data in the amide region of ν(NH) and ν(C═O) bands for the Fe(III) porphirin thiolate complexes, free ν(NH) and ν(C═O) of the corresponding disulfides, and the shift values. The amide ν(NH)s in **1**−**5** were observed over the region 3235−3331 cm^{-1} by a shift of 54−123 cm^{-1}. The corresponding ν(C═O) shifts are somewhat small (from −9 to −21 cm^{-1}) due to the free state of the amide C═O group. The combined data indicate the presence of the NH···S hydrogen bond. The strength of the NH···S hydrogen bond estimated by $\Delta\nu$(NH) shows the order of **3** > **1** > **4** > **5** > **2**. The trend depends on the number of NH···S hydrogen bonds and the electron-withdrawing substituent effect of the alkyl group of the amide.

^{1}H NMR Spectra. Table 4 lists the ^{1}H NMR chemical shifts of complexes **1**−**5**, compared with those of complexes [Fe^{III}(OEP)(SPh)] (**6**), [Fe^{III}(OEP)(S-2-$CH_3C_6H_4$)] (**7**), [Fe^{III}(OEP)(S-2,4,6-$Me_3C_6H_2$)] (**8**), and [Fe^{III}(OEP)(S-4-$CF_3CONHC_6H_4$)] (**9**) in benzene-d_6 at 30 °C. The ^{1}H NMR spectra of **3** and **9** are shown in Figures 3 and 4. The ^{1}H NMR signals of arenethiolate moiety in these Fe(III) porphyrin thiolate complexes appear at −93 to −96 ppm, assignable to 2,6-Ar−Hs; at 55−87 ppm, to 3,5-Ar−Hs; and at −83 to −94 ppm, to 4-Ar−H. On the other hand, the ^{1}H NMR signal of porphinate *meso*-H was observed at −41 to −47 ppm, and the α−CH_2 signal appears at 34−48 ppm. These chemical shifts are similar to those of the reported 5-coordinated high-spin Fe(III) porphinate complexes.[29,30] The ^{1}H NMR spectra of complex **8** (Figure S3) contain signals at 13, 33, and 75 ppm due to the β-CH_3, α-CH_2, and *meso*-H of [Fe^{II}(OEP)] as a reduced product.[31]

The observation of the ^{1}H NMR signal for 6-Ar−H on the arenethiolate ligand in **3**−**5** was difficult because the 6-Ar−H signal has an extremely small T_1 value due to the dipolar contact from high-spin Fe(III) ion. Only a broad signal of the 6-Ar−H was obtained even with the adoption of the short dead time and delay time. The Fe···H distances in **3** (6.012 Å for 3-Ar−H, 6.536 Å for 4-Ar−H, 5.676 Å for 5-Ar−H, and 3.761 Å for 6-Ar−H) were obtained by X-ray analysis and are shown in Figure 5. The assignments of these Ar−H signals were carried out on the basis of the relationship between the T_1 value and the Fe···H distance obtained from the crystal structure as obeying a reported relationship between them.[29]

Detection of Amide NH by ^{2}H NMR Spectra. For eluding the difficulty in the observation of the ^{1}H NMR signal for the amide NH of **1**−**5** in benzene-d_6 at 30 °C, we examined ^{2}H NMR for the detection of these amide signals. A clear amide N^{2}H signal was found in the ^{2}H NMR spectra of N^{2}H-substituted Fe(III) porphinate complexes **1**−**5** as shown in Figure 3a, and the ^{2}H chemical shifts of the amide N^{2}H are listed in Table 4. The ^{2}H NMR signals of amide N^{2}Hs in **1**−**4** were observed upfield in the region from −24 to −43 ppm. The sharp downfield-shifted ^{1}H NMR signal of amide NH in **9** was found at 30.4 ppm as well as the ^{2}H NMR signal at 29.6 ppm (Figure 4).

UV−Visible and ESR Spectra. The UV−visible spectra of **1**−**5** were measured at 0.15 mM concentration in benzene at room temperature. The absorption maxima and molar coefficient for **1**−**6** are listed in Table 5. The spectra of **1**−**5** indicate the typical 5-coordinated high-spin Fe(III) porphinate complexes.[15,32] The α, β, and Soret bands of **1**−**5** are observed at 643−651, 510−511, and 382−390 nm, respectively, whereas the α, β, and Soret bands of **6** are found at 636, 518, and 387 nm, respectively.

The ESR spectra of **1** and **3** were measured in toluene glass at 4.2 K. **1** and **3** exhibit *g* values at 6.7, 6.4, 5.1, and 2.0 and at 6.7, 6.0, 5.0, and 2.0, respectively (Figure S4). These values indicate that complexes **1** and **3** contain a 5-coordinated high-spin Fe(III) porphinate core in solution.[15]

(29) Arasasingham, R. D.; Balch, A. L.; Cornman, C. R.; Ropp, J. S. D.; Eguchi, K.; Mar, G. N. L. *Inorg. Chem.* **1990**, *29*, 1847−1850.
(30) Arasasingham, R. D.; Blach, A. L.; Hart, R. L.; Latos-Grazynski, L. *J. Am. Chem. Soc.* **1990**, *112*, 7566−7571.
(31) Stolzenberg, A. M.; Strauss, S. H.; Holm, R. H. *J. Am. Chem. Soc.* **1981**, *103*, 4763−4778.
(32) Ogoshi, H.; Sugimoto, H.; Yoshida, Z. *Tetrahedron Lett.* **1975**, *27*, 2289−2292.

Table 3. Detection of NH···S Hydrogen Bond Formation of [Fe^{III}(OEP)SAr] by IR in the Solid State (KBr Pellet)[a]

SAr	ν(NH)$_{complex}$	ν(NH)$_{free}$[b]	$\Delta\nu$(NH)[c]	ν(C=O)$_{complex}$	ν(C=O)$_{free}$	$\Delta\nu$(C=O)[d]
S-2,6-$(CF_3CONH)_2C_6H_3$ (**1**)	3278	3370	−92	1728	1747	−19
S-2,6-$(CH_3CONH)_2C_3H_3$(**2**)	3331	3385	−54	1687	1704	−17
S-2-$CF_3CONHC_6H_4$ (**3**)	3235	3358	−123	1722	1743	−21
S−2-$CH_3CONHC_6H_4$ (**4**)	3304	3382	−78	1692	1701	−9
S-2-*t*-$BuCONHC_6H_4$ (**5**)	3331	3397	−66	1676	1688	−12

[a] In cm^{-1}. [b] Free ν(NH) of the corresponding disulfide in CH_2Cl_2 (5−20 mM). [c] $\Delta\nu(NH) = \nu(NH)_{complex} - \nu(NH)_{free}$. [d] $\Delta\nu(C{=}O) = \nu(C{=}O)_{complex} - \nu(C{=}O)_{free}$.

Table 4. ^1H and ^2H NMR Chemical Shifts of Contact-Shifted Porphinate and Arenethiolate $^1H(^2H)$ NMR Signal for [Fe^{III}(OEP)(SAr)] in C_6D_6 at 30 °C

	chemical Shifts, ppm (T_1, ms)									
SAr	*meso*-H	α-CH_2		β-CH_3	2,6-H	3,5-H		4-H	NH	CH_3, *t*-Bu
S-2,6-$(CF_3CONH)_2C_6H_3$ (**1**)	−41.9	47.2	41.8	7.0		55.7		−83.2	−24.8[a]	
S-2,6-$(CH_3CONH)_2C_6H_3$ (**2**)	−44.1	43.2	41.0	6.6		61.8		−89.0	−34.3[a]	10.6
S-2-$CF_3CONHC_6H_4$ (**3**)	−45.8	42.3	39.7	6.5	−94.8 (0.12)	63.8 (1.8)	54.3 (1.4)	−86.1 (2.0)	−38.1[a]	
S-2-$CH_3CONHC_6H_4$ (**4**)	−45.5	40.1	38.8	6.3	−93.2	66.1	55.9	−88.2	−43.0[a]	9.8
S-2-*t*-$BuCONHC_6H_4$ (**5**)	−46.6	40.4	38.5	6.3	−95.9	69.5	56.4	−88.2	*b*	0.6
SPh (**6**)	−46.1	37.1	36.6	5.9	−95.5	60.2	−91.2			
S-2-$CH_3C_6H_4$ (**7**)	−46.0	37.1	35.9	6.0	*b*	86.9	75.1	−93.4		87.1
S-2,4,6-$CH_3C_6H_2$ (**8**)	−46.5	36.4	34.4							
S-4-$CF_3CONHC_6H_4$ (**9**)	−46.5	38.4	37.3	6.1	−95.3	57.8			30.4	

[a] Amide protons assigned by the 500 MHz ^2H NMR spectra for amide N^2H deuterated complexes. [b] Not detected.

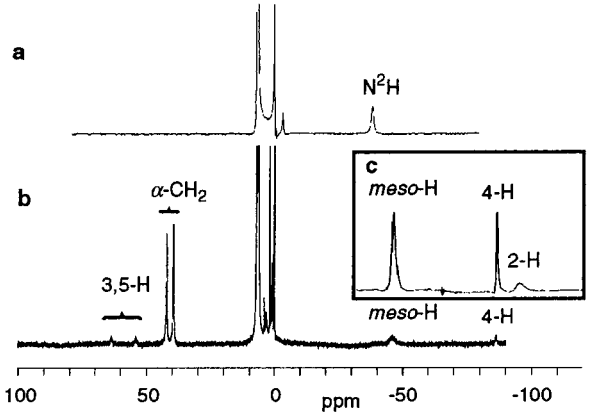

Figure 3. (a) ^2H NMR spectrum of [Fe^{III}(OEP)(S-2-$CF_3CON^2HC_6H_4$)] in benzene, (b) 270-MHz ^1H NMR spectrum of [Fe^{III}(OEP)(S-2-$CF_3CONHC_6H_4$)] (**3**) in benzene-d_6, and (c) 400-MHz ^1H NMR spectrum of **3** in benzene-d_6 at 30 °C.

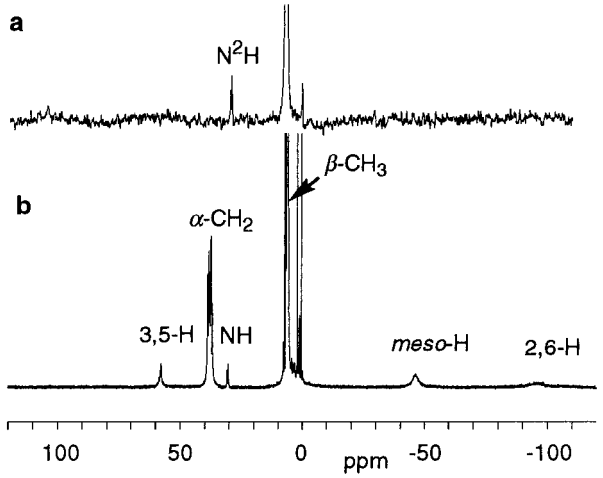

Figure 4. (a) ^2H NMR spectrum of [Fe^{III}(OEP)(S-4-$CF_3CON^2HC_6H_4$)] in benzene and (b) ^1H NMR spectrum of [Fe^{III}(OEP)(S-4-$CF_3CONHC_6H_4$)] (**9**) in benzene-d_6 at 30 °C.

Decomposition by Dioxygen. Typical Fe(III) porphinate thiolate complexes reported are unstable under air because dioxygen oxidizes thiolate to disulfide as shown in the following eq 3:[15]

$$2[Fe^{III}(OEP)(SAr)] + {}^1/_2O_2 \rightarrow [Fe^{III}(OEP)]_2O + ArSSAr \quad (3)$$

The decomposition of **1**−**5** and **6** to $[Fe^{III}(OEP)]_2O$ by 3000 equiv of dioxygen was monitored using a UV−visible spectroscopic method (Figure S5). The yields in the decomposition of these complexes after 1 h are illustrated in Figure 6. The order of stability is **1** > **3** > **5** > **2** > **4** > **6**. Especially **1** remains without any change in the absorption spectrum after 5 days. Thus, the formation of the NH···S hydrogen bond effectively prevents the thiolate ligand from dissociative oxidation.

We have tried to detect [Fe^{IV}=O$(OEP)^{+\bullet}$(SAr)] or [Fe^{IV}=O(OEP)(SAr)] species by the oxidation of **1** with PhIO or H_2O_2. However, the reactions gave $[Fe^{III}(OEP)]_2O$ and decomposed the ligand, respectively (Figure S6).

Electrochemical Properties. The cyclic voltammograms of **1**−**7** and **9** were obtained in 2.5 mM dichloromethane solution at room temperature. The typical cyclic voltammograms for **1** and **3** are shown in Figure S7. The redox potentials and reversibilities in the Fe^{III}/Fe^{II} couple of these complexes are listed in Table 6. The redox potentials of **1**−**5** show large positive shifts in the order of **1** > **2** > **3** > **4** > **5**. These values are shifted by 0.10−0.33 V from that (−0.68 V vs SCE) of [Fe^{III}(OEP)(SPh)] (**6**). On the other hand, 2-methyl (**7**) and 4-CF_3CONH (**9**) substituents show very small contributions to the redox potential without the NH···S hydrogen bond. Thus, clearly the NH···S hydrogen bond contributes to the positive shift of the redox potential.

However, the reversibility for the redox couple is small, as shown in Table 6. The observed low I_{pa}/I_{pc} of 0.40−0.68 indicates instability of the reduced Fe(II) state. Actually, the isolation of any Fe(II) species was unsuccessful after reduction of **5** with NEt_4BH_4.

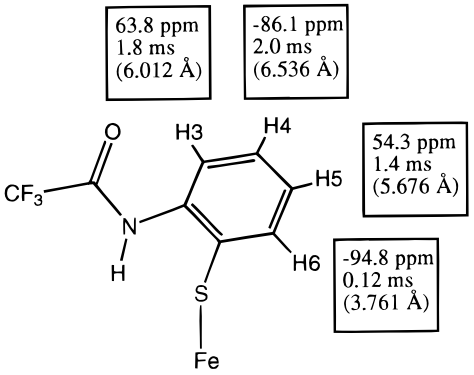

Figure 5. Contact shifts and their T_1 values of ^{1}H NMR signals of the benzenethiolate ligand in [Fe^{III}(OEP)(S-2-$CF_3CONHC_6H_4$)] (**3**). The parentheses represent the Fe- - -H distances obtained from the X-ray crystal analysis.

Table 5. Absorption Spectral Data in the Porphinate Region for [Fe^{III}(OEP)(SAr)] in Benzene

	$\lambda_{max}{}^a$ ($\epsilon \times 10^{-3}$)^b		
SAr	α	β	Soret
S-2,6-$(CF_3CONH)_2C_6H_3$ (**1**)	650 (3.8)	510 (13)	382 (110)
S-2,6-$(CH_3CONH)_2C_6H_3$ (**2**)	651 (4.5)	511 (15)	390 (96)
S-2-$CF_3CONHC_6H_4$ (**3**)	644 (5.6)	510 (15)	382 (120)
S-2-$CH_3CONHC_6H_4$ (**4**)	644 (6.2)	511 (17)	388 (120)
S-2-*t*-$BuCONHC_6H_4$ (**5**)	643 (6.2)	510 (17)	389 (110)
SPh (**6**)	636 (5.8)	518 (13)	387 (100)

^{a} In nm. ^{b} In M^{-1} cm^{-1}.

Discussion

Elongation of Fe−S Bond Distance by NH···S Hydrogen Bond. The crystal structures of [Fe^{III}(OEP){S-2,6-$(CF_3CONH)_2C_6H_3$}] (**1**) and [Fe^{III}(OEP)(S-2-$CF_3CONHC_6H_4$)] (**3**) indicate the presence of the NH···S hydrogen bond on the basis of the orientation of the amide NH to the sulfur atom. The N···S distance of **3** is shorter by 0.03 Å than that of **1**, and the difference of the (N)H···S distance is 0.03−0.04 Å. This fact is ascribed to the formation of a stronger NH···S hydrogen bond in **3** than in **1**. The results are consistent with the conclusion from the shift of IR ν(NH) band.

The Fe−S bond distance elongates proportional to the number of the NH···S hydrogen bonds. It is likely that the NH···S hydrogen bond decreases π donation of sulfur to iron. We have previously reported the shortening of the M−S bond by the NH···S hydrogen bond when the HOMO involves antibonding M−S interaction.[24,33,34] In the porphyrin complexes, the HOMO is mainly on the porphyrin ligand; thus the decrease in π donation ability predominantly contributes to the elongation of the Fe−S bond.

Change in the Strength of NH···S Hydrogen Bond by the Electronic Effect of Acylamide Substituent. The extent of the $\Delta\nu$(NH) shift reflects the strength of the NH···S hydrogen bond in the order **3** > **1** > **4** > **5** > **2**. Thus, the electron-withdrawing group, for example, CF_3, strengthens the hydrogen bond. The trend **3** > **4** > **5**, i.e., CF_3 > CH_3 > *t*-Bu, agrees with the electron-withdrawing ability. A stronger NH···S hydrogen bond exists for the single amide NH in **3** than for each of two amide NHs in **1**. On the other hand, the order in the oxidative decomposition against dioxygen and that in the redox potential of these complexes are **1** > **3** > **5** > **2** > **4** and **1** > **2** > **3** > **4**, **5**, respectively. The strength and number of the NH···S hydrogen bond are found to contribute to the positive shift of the redox potential as previously reported for iron−sulfur complexes.[21]

The positive shift of the redox potentials is greater with two NH···S hydrogen bonds. Oxidative decomposition is presumably initiated by an attack of molecular oxygen, also accompanied by dissociation of Fe−S to give disulfide. The dissociation of Fe−S is facilitated by protonation of the sulfur by a trace amount of water. The CF_3 group decreases the electron density on the sulfur resulting in a positive shift of the reduction potential of the disulfide and an increase in the acidity of the thiol. In both cases, the Fe−S bond is stabilized. The bulkiness or hydrophobic environment of the *t*-Bu group likely protects the Fe−S bond from the attack of oxygen or water. Consequently, the order of CF_3 > *t*-Bu > CH_3 is observed in the oxidative decomposition of [Fe^{III}(OEP)(SAr)].

The porphinate α band in the visible absorption spectra of **1**−**5** redshifts depending on the strength of the NH···S hydrogen bond. A similar shift has been observed for some of the OEP Fe(III) complexes by Uno et al.[35] They discussed a correlation between the shift and pK_a value of *p*-substituted phenol at the

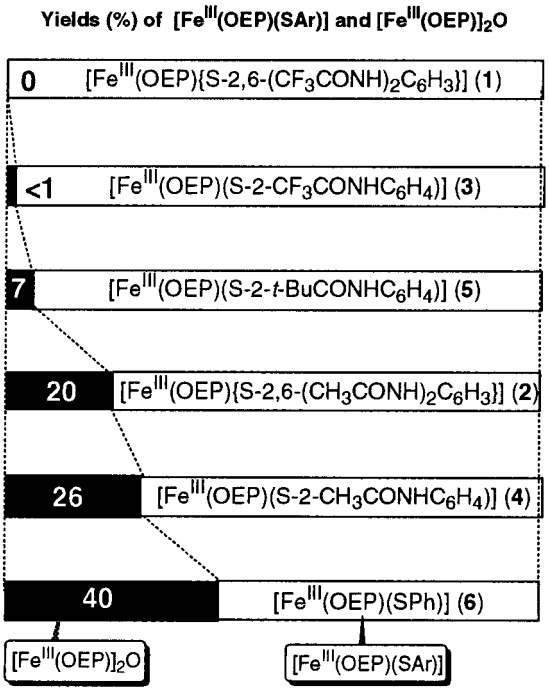

Figure 6. Amounts (%) of producing [Fe^{III}(OEP)]$_2$O from [Fe^{III}(OEP)(SAr)] upon exposure to air for 1 h.

Table 6. Electrochemical Data of Fe(III) Porphyrin Thiolate Complex, [Fe^{III}(OEP)(SAr)]

SAr	$E_{1/2}{}^a$	$E_{pc}{}^a$	$E_{pa}{}^a$	I_{pa}/I_{pc}
S-2,6-$(CF_3CONH)_2C_6H_3$ (**1**)	−0.35	−0.46	−0.24	0.61
S-2,6-$(CH_3CONH)_2C_6H_3$ (**2**)	−0.50	−0.60	−0.40	0.40
S-2-$CF_3CONHC_6H_4$ (**3**)	−0.52	−0.61	−0.43	0.66
S-2-$CH_3CONHC_6H_4$ (**4**)	−0.58	−0.65	−0.51	0.68
S-2-*t*-$BuCONHC_6H_4$ (**5**)	−0.58	−0.66	−0.50	0.68
SPh (**6**)	−0.68	−0.74	−0.63	0.67
S-2-$CH_3C_6H_4$ (**7**)	−0.72	−0.76	−0.68	0.66
S-4-$CF_3CONHC_6H_4$ (**9**)	−0.67	−0.73	−0.60	0.55

^{a} In V vs SCE in dichloromethane.

(33) Ueyama, N.; Okamura, T.; Nakamura, A. *J. Am. Chem. Soc.* **1992**, *114*, 8129−8137.
(34) Ueyama, N.; Okamura, T.; Nakamura, A. *J. Chem. Soc., Chem. Commun.* **1992**, 1019−1020.
(35) Uno, T.; Hatano, K.; Nishimura, Y.; Arata, Y. *Inorg. Chem.* **1990**, *29*, 2803−2807.

axial position of OEP. The decrease in the pK_a results in the red shift of the α band. Thus the α bands of **1**−**5** red shift by 7−14 nm compared with that of benzenethiolate complex **6** which has no NH···S hydrogen bond. Because the NH···S hydrogen bond stabilizes the thiolate state, the thiols having a neighboring NH group are expected to have lower pK_a values.[28]

Contact Shift of ^{1}H or ^{2}H NMR Signal by High-Spin Fe(III) Ion. There has been no report on the ^{1}H NMR spectra in the active center region for the high-spin Fe(III) state of cytochrome P-450s, although the detection has been attempted.[36] When the ^{1}H NMR signals of the amide protons associated with the NH···S hydrogen bond in these model complexes are assigned, the strength of the hydrogen bond, the closely related Fe^{III}−S bond character and the nature of the active site in the Fe(III) state of the P-450s will be elucidated. However, the proton signals could not be observed because the signals are too broad due to the extremely small T_1 value by a direct through-bonding Fe−S···HN interaction via the NH···S hydrogen bond. In contrast, the deuterated amide N^{2}H signals of these model complexes are successfully observed as shown in Table 5. Generally, the amide NH ^{1}H NMR signal at 2-Ar−H of arenethiolate appears downfield as well as the 2-Ar−H and the 4-amide NH of 4-acylamide complex **9** obeying a conjugated π-spin rule. However, the amide NH signal at the 2-position of **3** is observed to be upfield at −38.1 ppm and that in **9** to be upfield at +30.4 ppm. This shift comes from a direct through-bonding Fe−S···HN contact with a direct interaction through the NH···S hydrogen bond. Furthermore, the contact shift is larger than those (−12.9 and 5.3 ppm) of the contact-shifted amide NH ^{1}H NMR signals of $[Co^{II}(S\text{-}2\text{-}t\text{-}BuCONHC_6H_4)_4]^{2-}$ and $[Co^{II}(S\text{-}4\text{-}t\text{-}BuCONHC_6H_4)_4]^{2-}$, respectively.[24,34]

Positive Shift of the Redox Potential by the Specific NH···S Hydrogen Bond. The NH···S hydrogen bond shifts the redox potential to the positive side with the order of **1** > **2** > **3** > **4**, **5** > **9** > **6** > **7** in dichloromethane. As the number and the strength of the NH···S hydrogen bonds increase, the redox potential increasingly shifts to more positive potential. For example, $[Fe^{III}(OEP)\{S\text{-}2,6\text{-}(CF_3CONH)_2C_6H_3\}]$ (**1**) has an extremely positive-shifted redox potential at −0.35 V vs SCE compared with −0.67 V vs SCE of the non-hydrogen bonded one, $[Fe^{III}(OEP)(S\text{-}4\text{-}CF_3CONHC_6H_4)]$ (**9**). In this case, the electronic effect by ortho and para substituents is not significant because the small difference (0.01−0.05 V) in the redox potential among **6**, **7**, and **9** indicates only a very weak electronic effect of the para substituent in accord with their Hammett σ_p constant (CH_3CONH = 0, CF_3CONH = 0.12).[27]

In native P-450 enzymes, the redox potentials were reported to be at −0.415 V vs SCE for substrate-binding P-450cam and at −0.572 V vs SCE for nonsubstrate-binding P-450cam.[18] Furthermore, the structures from both crystallographic analyses[2,37] suggest the presence of NH···S hydrogen bonds near the active center, especially in the substrate-binding state. The N···S distances are 3.25 and 3.40 Å for substrate bound and 3.45 and 3.42 Å for substrate free P-450 based on the crystal data.[2,37] The difference of N···S distances is considered to significantly contribute to the positive shift of the redox potential as well as our results of the model complexes.

Previously, the origin for the positive shift of the redox potential has been proposed to be the structural change from the Fe(III) low-spin state with a water molecule to the Fe(III) high-spin state without the water molecule.[18] However, the large positive shift of the redox potential by the NH···S hydrogen bond in the P-450 model complexes implies that the regulation of the redox potential in P-450s is mainly performed by the specific hydrogen bond between the Cys sulfur and the neighboring peptide amide NH.

Stabilization of Fe(III) State by NH···S Hydrogen Bond. The remarkable stability of the visible spectrum of complex **1** upon exposure to dioxygen for 5 days indicates an extreme stability of the Fe(III) state in dichloromethane. The stability is thus ascribed to the double NH···S hydrogen bonds. The increase in the pK_a of the thiol prevents the Fe(III)-thiolate bond from dissociation of the thiolate ligand in an aqueous medium. Complex **1** can thus exist as a stable thiolate complex in an aqueous micellar solution.

On the other hand, a low reversibility of the Fe^{III}/Fe^{II} couple shows the instability of the reduced Fe(II) species in dichloromethane. The ease in one-electron reduction of the Fe(III) state in native cytochrome P-450 is crucial for the following oxidation of the reduced state with dioxygen. The reduction of **1** with tetraethylammonium borohydride readily occurs to give an Fe(II) state which rapidly decomposes under ambient conditions. Thus, the NH···S hydrogen bond does not contribute to the kinetic stabilization of the Fe(II) species.

Acknowledgment. Support of this work by a Grant-in-Aid for Specially Promoted Research (06101004) from the Ministry of Education, Science and Culture of Japan is gratefully acknowledged.

Supporting Information Available: ORTEP drawing of **1** and **3** (Figure S1), NMR spectra of **1** and **8** (Figures S2 and S3), ESR spectra of **1** and **3** (Figure S4), UV−visible spectra of the oxidation reaction of **4** and **1** (Figures S5 and S6), and cyclic voltammograms of **1** and **3** (Figure S7) are available (7 pages). X-ray crystallographic files in CIF format for the structure determination of **1** and **3** are available on the Internet only (see ref 22 (JA9622970)). Ordering or access information is given on any current masthead page.

IC971140L

(36) Lukat, G. S.; Goff, H. M. *Biochim. Biophys. Acta* **1990**, *1037*, 351−359.

(37) Poulos, T. L.; Finzel, B. C.; Gunsalus, I. C.; Wagner, G. C.; Kraut, J. *J. Biol. Chem.* **1985**, *260*, 16122−16130.